
Elastic Architecture Search for Diverse Tasks with Different Resources

Jing Liu¹, Bohan Zhuang^{1†}, Mingkui Tan^{2†}, Xu Liu²,
Dinh Phung¹, Yuanqing Li², Jianfei Cai¹

¹ Dept of Data Science and AI, Monash University

² South China University of Technology

Abstract

We study a new challenging problem of efficient deployment for diverse tasks with different resources, where the resource constraint and task of interest corresponding to a group of classes are dynamically specified at testing time. Previous NAS approaches seek to design architectures for all classes simultaneously, which may not be optimal for some individual tasks. A straightforward solution is to search an architecture from scratch for each deployment scenario, which however is computation-intensive and impractical. To address this, we present a novel and general framework, called Elastic Architecture Search (EAS), permitting instant specializations at runtime for diverse tasks with various resource constraints. To this end, we first propose to effectively train the over-parameterized network via a **task dropout** strategy to disentangle the tasks during training. In this way, the resulting model is robust to the subsequent task dropping at inference time. Based on the well-trained over-parameterized network, we then propose an efficient architecture generator to obtain optimal architectures within a single forward pass. Experiments on two image classification datasets show that EAS is able to find more compact networks with better performance while remarkably being orders of magnitude faster than state-of-the-art NAS methods. For example, our proposed EAS finds compact architectures within 0.1 second for 50 deployment scenarios.

1 Introduction

Deep neural networks (DNNs) have achieved state-of-the-art performance in many areas in machine learning [16, 46] and much broader artificial intelligence. There are a great number of practical applications where we need a well-trained general model (capable of classifying thousands of classes) to be flexible during deployment (e.g., focusing on classifying tens of classes), as shown in Figure I. For example, zoologists might only be interested in classifying the categories like cat, dog, and so on, while a large number of other classes provided by a deep classifier is useless to them. Moreover, in reality, we usually need to deploy models to diverse platforms with different resource constraints (e.g., latency, energy, memory). Besides, the computational budget varies due to the consumption of background apps that reduces the available computing capacity, and the energy budget varies due to the decreasing battery level of a mobile phone. This gives rise to a new challenge: how to instantly find an accurate and compact architectural configuration, given a specified task of interest and resource budget at runtime.

To obtain compact architectures, most existing approaches either manually design [20, 49] or use compression methods [36, 66, 65] and neural architecture search [67, 4, 3] to find a specialized

[†]Corresponding author.

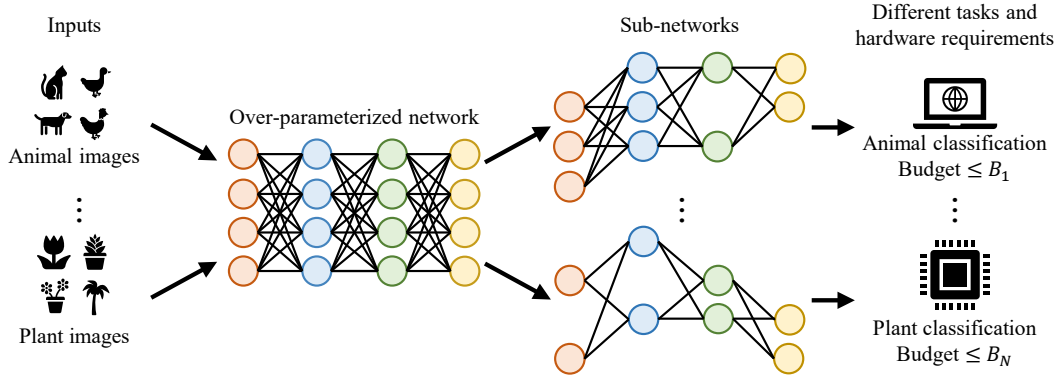


Figure I: An illustration of diverse application scenarios for different tasks under various resource budgets. For different deployment scenarios, the optimal architectures are different.

network. However, they all assume that all the tasks (each task corresponds to a group of classes) are predicted at the same time, which limits the flexibility. In particular, for different tasks (e.g., animal classification and plant classification), the optimal architectures can differ a lot. It is extremely time-consuming and computation-intensive to repeatedly retrain the network to find the architectures for each task, as the training cost grows linearly with the number of possible cases, and there are vast varieties of devices and dynamic deployment environments, which further exacerbate the efficiency problem significantly.

To address the above issue, one may consider the one-shot NAS methods [2, 61] to decouple the model training and the architecture search stage, where different sub-networks can be extracted from a trained over-parameterized network without any retraining. However, existing one-shot NAS methods suffer from two limitations. First, they ignore disentangling the tasks during the model training stage, which is not straightforward to adapt to arbitrary task specifications during deployment. Second, existing one-shot NAS methods learn a surrogate model to estimate the model accuracy of the architecture and then use evolutionary algorithm [2] or coarse-to-fine strategy [61] to find optimal architectures during the deployment stage. Nevertheless, training a surrogate model requires plenty of architectures with the ground-truth accuracy which are time-consuming to collect (e.g., 40 GPU hours to collect 16K sub-networks in OFA [2]). Moreover, for M requirements of different tasks with diverse resources, existing methods have to search for M times, which is inefficient and unnecessary. To tackle the above challenges, this paper introduces a novel and general framework, called Elastic Architecture Search (EAS), to deliver instant and effective trade-offs between accuracy and efficiency to support diverse tasks of interest under different hardware constraints. In particular, the proposed EAS trains an over-parameterized network that supports many sub-networks and generates the architectures on the fly according to arbitrary deploying scenarios. To this end, we propose a task dropout strategy that randomly drops the output logits corresponding to different tasks during training. In this way, the over-parameterized network is robust to the task specification at testing time. To enable specialization to arbitrary tasks with different resources, we further propose an architecture generator to obtain architectures within a single forward pass, which is extremely efficient.

Our main contributions are summarized as follows:

- We study a practical deep model deployment task for diverse tasks of interest with arbitrary hardware resources. To our best knowledge, this task has not received enough attention from the community. To resolve this, we devise a novel framework, called Elastic Architecture Search (EAS), which supports versatile architectural configurations for many different deployment requirements at runtime.
- We propose a task dropout strategy to disentangle the tasks during the over-parameterized network training, making the network robust to the subsequent task specification during deployment. We further design an efficient architecture generator to directly generate architectures without the need to search from scratch for each deployment scenario, which greatly reduces the specialization cost.

- Experiments on two image classification datasets show the superior performance and efficiency of the proposed EAS. For example, our proposed EAS is able to find accurate and compact architectures within 0.1 second for 50 deployment scenarios.

2 Related work

Network compression. Network compression aims to reduce the model size and speed up the inference without significantly deteriorating the model performance. Existing network compression methods can be divided into several categories, including but not limited to network pruning [36, 31, 11, 30], network quantization [64, 65, 9, 26], knowledge distillation [47, 17, 63, 37], low-rank decomposition [7, 23, 62, 38], etc. Although achieving promising performance, prevailing methods only target predicting all the classes simultaneously. For different groups of classes (i.e., tasks) of interest, it requires repeatedly retraining to find a compact network, which is time-consuming and inefficient. In contrast, our proposed EAS trains an over-parameterized network that supports a huge number of sub-networks for diverse tasks with different resources.

Neural architecture search (NAS). NAS seeks to design efficient architectures automatically instead of relying on human expertise. Existing NAS methods can be roughly divided into three categories according to the search strategy, namely, reinforcement learning-based methods [67, 39, 52, 13], evolutionary methods [43, 34, 42, 33], and gradient-based methods [3, 29, 56, 22]. When it comes to different resource constraints, these methods have to repeatedly train the network and search for optimal architectures. To solve this problem, one-shot NAS methods [2, 15, 61] have been proposed to train a once-for-all (OFA) network that supports different architectural configurations by decoupling the model training stage and the architecture search stage. To search for optimal architectures efficiently, one can use evolutionary search [2] or design an architecture generator to obtain effective architectures [59, 48]. However, given different resource constraints, these methods have to search architectures for each deployment scenario, which is inefficient. Unlike these methods, we propose an efficient architecture generator that is able to obtain architectures on the fly given diverse tasks with different resource constraints within a forward pass.

Dynamic neural networks. Dynamic neural networks, as opposed to static ones, is able to adapt their structures or parameters to different inputs during inference and therefore enjoy the desired trade-off between accuracy and efficiency. Existing methods can be roughly divided into three categories according to the granularity of dynamic networks, namely, instance-wise [5, 21, 28, 54], spatial-wise [45, 55, 44] and temporal-wise dynamic networks [58, 10, 57]. However, the inference efficiency of the data-dependent dynamic networks relies on the largest activated network in a batch of data, which limits the degree of practicality. Moreover, all the above methods perform predictions for all tasks simultaneously. Unlike these methods, our proposed EAS is able to derive compact and accurate architectures given arbitrary tasks and efficiency constraints.

3 Elastic architecture search

Notation. Let $\mathcal{D}^t = \{(\mathbf{x}_n^t, y_n^t)\}_{n=1}^{N^t}$ be the training data for t -th task, where $\mathbf{x}_n^t \in \mathcal{X}^t$, $y_n^t \in \mathcal{Y}^t$, and N^t is the number of images. For simplicity, different tasks of data are disjoint and focus on different classes, namely, $\forall i, j \in \{1, \dots, T\}$ and $i \neq j$, $\mathcal{Y}^i \cap \mathcal{Y}^j = \emptyset$, and $D^i \cap D^j = \emptyset$. Let $\mathcal{D} = \{(\mathbf{x}_n, y_n)\}_{n=1}^N = \cup_{t=1}^T \mathcal{D}^t$ be the union of data for T tasks, where $N = \sum_{t=1}^T N^t$.

In this paper, we focus on the neural architecture search problem that aims to obtain architectures given arbitrary tasks with different resource budgets. To address this, one may use the existing NAS methods [39, 3] to search architectures for each task and resource budget. However, when it comes to a vast amount of tasks with various resource requirements, designing a specialized network for every scenario is computationally expensive and impractical.

To handle diverse tasks with different resource budgets dynamically during testing, we propose a novel method, called Elastic Architecture Search (EAS). Specifically, our proposed EAS trains an over-parameterized network on \mathcal{D} that supports a very large number of sub-networks. However, the training of the over-parameterized network is a highly entangled bi-level optimization problem [29]. Inspired by one-shot NAS [2, 61, 15], our solution is to decouple the model training stage and the architecture search stage. To make the model robust to the subsequent task specification during inference, we present a task dropout strategy at training time (See Section 3.1). Once the over-

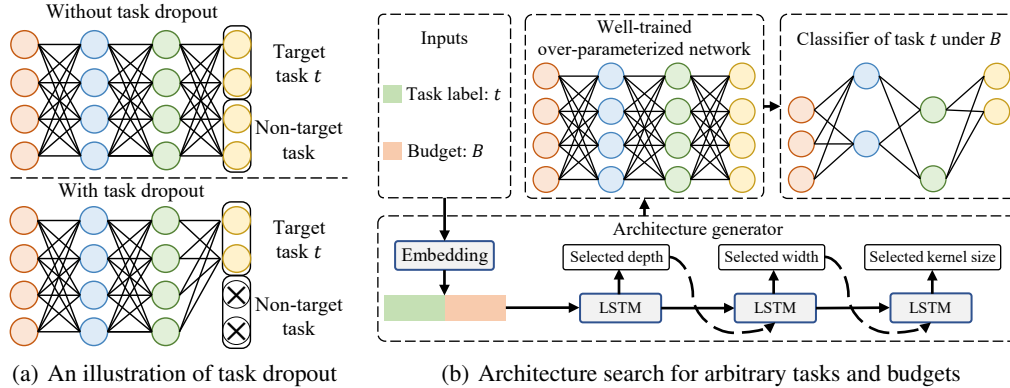


Figure II: The overview of the task dropout and architecture search. (a) We apply task dropout which randomly drops the output logits corresponding to the different tasks during the training of the over-parameterized network. (b) We build an architecture generator, which takes a task label t and resource budget B as inputs and generates architectures that satisfy the requirement. We use an embedding layer to map the task label and budget to the concatenated embedding vector.

parameterized network has been well-trained, we are able to search architectures for different tasks with various resources without any retraining. In particular, we propose an efficient architecture generator to obtain optimal architectures within one forward pass (See Section 3.2).

3.1 Task dropout for training over-parameterized network

Following [2], the over-parameterized network consists of many sub-networks with different depths, width expansion ratios, and kernel sizes, where the weights of small sub-networks are shared with large sub-networks. To prevent interference between different sub-networks, we use the progressive shrinking strategy to train the over-parameterized network following [2]. However, existing methods ignore disentangling the tasks as these methods train the over-parameterized network on \mathcal{D} that is the union of data for all tasks. As a result, the sub-networks may not be optimal for each \mathcal{D}^t . To achieve better performance, one may train an over-parameterized network for each \mathcal{D}^t separately, which is computationally expensive and impractical. Such method also ignores that the data from other tasks may contain useful context information for the target task, which may result in sub-optimal performance of the sub-networks.

To resolve these issues, motivated by [18, 53], we propose to train an over-parameterized network on \mathcal{D} with the task dropout strategy that randomly drops the output logits corresponding to non-target tasks at each step of optimization, as shown in Figure 2(a). Formally, let $\mathbf{v}_n \in \mathbb{R}^d$ be the input feature of the last fully connected layer corresponding to \mathbf{x}_n , where d is the input feature dimension. For convenience, we omit the sample index n . The output logits of the network, denoted by \mathbf{o} , can be computed by $\mathbf{o} = \mathbf{w}^\top \mathbf{v}$, where $\mathbf{w} \in \mathbb{R}^{d \times C}$ denotes the classifier’s weights of the last fully connected layer and C is the number of classes. To encode the dropping decision of classes corresponding to different tasks, we introduce a binary mask $\mathbf{m} \in [0, 1]^C$ to the output logits of the network:

$$\hat{\mathbf{o}} = \mathbf{m} \odot \mathbf{o}, \quad (\text{A})$$

where \odot is the operation of element-wise product and $\hat{\mathbf{o}}$ is the masked version of \mathbf{o} . Without any constraint, Eq. (A) is a form of class dropping. To engage task dropping, the binary mask \mathbf{m} must be organized into groups by $\mathcal{G} = \{G^1, \dots, G^T\}$, where $\cup_{t=1}^T G^t = \{1, \dots, C\}$, $G^i \cap G^j = \emptyset$ for $\forall i, j$ and $i \neq j$, and G^t denotes the index set of binary mask belonging to the t -th group. In this case, the output logits of the t -th task are

$$\hat{\mathbf{o}}_{G^t} = \mathbf{m}_{G^t} \odot \mathbf{o}_{G^t}, \quad (\text{B})$$

where $\hat{\mathbf{o}}_{G^t}$, \mathbf{m}_{G^t} and \mathbf{o}_{G^t} are the t -th group components of $\hat{\mathbf{o}}$, \mathbf{m} and \mathbf{o} , respectively. Here, the binary mask \mathbf{m}_{G^t} controls the dropping decision of the task t . During the model training stage, for any sample $(\mathbf{x}^t, y^t) \in \mathcal{D}^t$ in a batch of data, the components of $\hat{\mathbf{o}}$ corresponding to the non-target tasks (i.e., $\forall j \in \{1, \dots, T\}$ and $j \neq t$) are randomly dropped following a Bernoulli distribution with a

hyper-parameter $q \in [0, 1]$ that controls the drop rate. In this way, the over-parameterized network is robust to the subsequent task dropping at testing time.

3.2 Architecture search for arbitrary tasks with different resources

Once the over-parameterized network has been well-trained, we now focus on how to quickly find a specialized sub-network from the over-parameterized network given arbitrary deployment scenarios. To find optimal architectures, one may train a surrogate model to learn the mapping from an architectural configuration to its accuracy and then use evolutionary algorithm [2] or coarse-to-fine strategy [61] to explore the large configuration space. However, training such a surrogate model requires plenty of architecture-accuracy pairs that are very expensive to obtain in practice (e.g., 40 GPU hours to collect 16K sub-networks in OFA [2]). Moreover, for different tasks with various resource budgets, existing methods have to search architectures for each deployment scenario, which is extremely inefficient and unnecessary.

To solve the above issue, we propose an architecture generator model to obtain architectures for diverse tasks with different resources within a single forward pass. As shown in Figure 2(b), the architecture generator $G(B, t; \theta)$ is based on an LSTM network with three fully connected layers following [39]. Here, θ is the parameters of the architecture generator. Specifically, $G(B, t; \theta)$ takes a resource budget B and task label t as input and generates the architecture encoding α . Following [39, 14], we define K budgets evenly sampled from the range of $[B_L, B_H]$, where B_L and B_H are the minimum and maximum of resource budgets respectively. To represent different tasks and budgets, we build learnable embedding vectors for each of the task labels and predefined budgets. To deal with a resource budget with an arbitrary value, we use an embedding interpolation method following [12, 41]. We then concatenate the resulting budget and task embedding vectors and feed them into the LSTM network. By incorporating the learnable embedding vectors into the parameters of the architecture generator, we are able to train them jointly. The training details of the proposed architecture generator are shown in Algorithm 1.

Objective function. The goal of the architecture generator is to obtain an architecture encoding α corresponding to a sub-network from the well-trained over-parameterized network that minimizes the validation loss $\mathcal{L}_{\text{val}}(\mathbf{W}, \alpha)$, where \mathbf{W} is the weights of the over-parameterized network. Here, the validation loss is the cross-entropy on the validation set. To ensure that the computational cost $R(\alpha)$ is close to B , we introduce a computational constraint loss, which can be formulated as

$$\mathcal{L}_C(\alpha, B) = (R(\alpha) - B)^2. \quad (\text{C})$$

By considering both the validation loss and computational constraint loss, the joint loss function can be formulated as

$$\mathcal{L}(\theta) = \mathcal{L}_{\text{val}}(\mathbf{W}, G(B, t; \theta)) + \lambda \mathcal{L}_C(G(B, t; \theta), B), \quad (\text{D})$$

where λ is a hyper-parameter that balances the two loss functions.

Single-path architecture encoding. Finding a sub-network from the well-trained over-parameterized network is a discrete and non-differentiable process [29, 3]. To efficiently explore the enormous search space of the well-trained over-parameterized network and optimize α using the gradient-based methods, existing multi-path-based NAS methods [56, 22] relax the search space to be continuous and formulate optimization as a path selection problem. In this case, the generated architecture is encoded by the path weights of the candidate modules. However, to find optimal architectures, these methods have to traverse all candidate paths, which leads to high memory footprint and computational cost. To address this, one may use a single-path framework [50, 51] to encode architectural configurations (i.e., kernel size and width expansion ratio) in the search space of the well-trained over-parameterized network and formulate the NAS problem as a subset selection problem. In this case, the architecture encoding α can be represented by a series of binary gates that determine which subset of weights to use and the computational cost $R(\alpha)$ is a function of the binary gates.

Apart from the kernel size and width expansion ratio configurations introduced in the single-path NAS [50, 51], our over-parameterized network also supports elastic depth following OFA [2]. Basically, a shallower network can be viewed as the subsets of layers of the whole network. Therefore, the depth configuration can also be determined by a set of binary gates. Formally, let $\mathcal{H}^l(\mathbf{x})$ be the mapping until the l -th module and $\mathcal{F}(\cdot)$ be the mapping of the $(l + 1)$ -th module. Note that a module can be a layer or a block that consists of a collection of successive layers. Then, the mapping $\mathcal{H}^{l+1}(\mathbf{x})$

Algorithm 1 Training method for the architecture generator.

Require: The parameters of the well-trained over-parameterized network \mathbf{W} , minimum of the resource budget B_L , maximum of the resource budget B_H , uniform distribution $U(B_L, B_H)$, total task number T , task index set $\{1, \dots, T\}$, learning rate η , training data set $D = \cup_{t=1}^T \mathcal{D}^t$, hyper-parameters λ and τ .

- 1: Initialize the architecture generator parameters θ .
- 2: **while** not converged **do**
- 3: Randomly select a task label t from $\{1, \dots, T\}$.
- 4: Sample a batch of data from \mathcal{D}^t .
- 5: Sample a resource budget B from $U(B_L, B_H)$.
- 6: Compute the loss using Eq. (D).
- 7: Update the architecture generator by
- 8: $\theta \leftarrow \theta - \eta \nabla_{\theta} \mathcal{L}(\theta)$.
- 9: **end while**

until the $(l + 1)$ -th module can be formulated as

$$\mathcal{H}^{l+1}(\mathbf{x}) = \mathcal{H}^l(\mathbf{x}) \cdot (1 - g^{l+1}) + \mathcal{F}(\mathcal{H}^l(\mathbf{x})) \cdot g^{l+1}, \quad (\text{E})$$

where g^{l+1} is a binary gate to determine whether to go through the $(l + 1)$ -th module during the forward propagation. In this case, the computational cost R^{l+1} until the $(l + 1)$ -th module is

$$R^{l+1} = R^l + r^{l+1} \cdot g^{l+1}, \quad (\text{F})$$

where r^{l+1} is the computational cost of the $(l + 1)$ -th module.

Instead of determining the output of the binary gates using some heuristic metrics (e.g., the ℓ_1 -norm of the weights), we force the output of each binary gate following the Bernoulli distribution with a probability p_i , where i denotes the index of the binary gates. Formally, the output of the i -th binary gate can be computed by

$$g(p_i) = \begin{cases} 1 & \text{with probability } p_i, \\ 0 & \text{with probability } 1 - p_i. \end{cases} \quad (\text{G})$$

Therefore, the architecture encoding α is encoded by a set of binary gates and each binary gate is sampled from the Bernoulli distribution. To obtain p_i , we apply a sigmoid function $\sigma(\cdot)$ to the output \mathbf{z} of the LSTM network, which can be formulated as

$$p_i = \sigma(z_i), \quad (\text{H})$$

where z_i is the i -th element of \mathbf{z} .

Gumbel-Softmax for differentiable relaxation. To train the architecture generator, we need to estimate the gradient of the objective function $\mathcal{L}(\theta)$ w.r.t. the probability p_i . However, Eq. (G) is not differentiable w.r.t. p_i . Following [27], we use the Gumbel-Softmax reparameterization trick [35, 24] to reparameterize p_i as

$$h(p_i, \tau) = \sigma \left(\left(\log \frac{p_i}{1 - p_i} + \log \frac{u_i}{1 - u_i} \right) / \tau \right), \quad u_i \sim U(0, 1), \quad (\text{I})$$

where u_i is the random noise sampled from the uniform distribution $U(0, 1)$ and τ is the temperature hyper-parameter. During the forward propagation, the output of a binary gate is computed by

$$\hat{g}(p_i) = \begin{cases} 1 & \text{if } h(p_i, \tau) > 0.5, \\ 0 & \text{otherwise,} \end{cases} \quad (\text{J})$$

where $\hat{g}(p_i)$ is the hard version of $h(p_i, \tau)$. During backward propagation, we use straight-through estimator (STE) [1, 64] to approximate the gradient of $\hat{g}(p_i)$ by the gradient of $h(p_i, \tau)$. In this way, the objective function $\mathcal{L}(\theta)$ is differentiable w.r.t. p_i and we are able to train the architecture generator using gradient-based methods.

Inferring architectures for diverse tasks with different resources. Once the architecture generator has been trained, we can instantly search for a sub-network that meets a specific deployment scenario. Specifically, given a task label and resource budget, the output of the architecture generator is the probabilities of the binary gates encoding the architectural configurations. Thus, we can sample several architectures from the Bernoulli distributions. We will repeat the sampling process if the sampled ones violate the resource budget. Last, we select the final architecture with the highest validation accuracy. Moreover, our proposed architecture generator is able to generate architectures for M deployment requirements within a single forward pass by setting the mini-batch size to M .

Table I: Comparisons on ImageNet-10. We report the Top-1 Accuracy (Acc.) of different architectures on diverse tasks. “T- t ” indicates the t -th task. “Avg. Acc.” and “Avg. #MAdds” denote the average Top-1 accuracy and the average number of multiply-adds, respectively.

Method	T-1	T-2	T-3	T-4	T-5	T-6	T-7	T-8	T-9	T-10	Avg. Acc. (%)	Avg. #MAdds (M)
OFA-V	86.7	90.7	79.7	81.0	85.0	89.0	82.0	96.0	92.7	96.7	87.9	230
OFA-T	86.3	90.0	79.7	79.0	85.3	87.3	83.0	97.0	93.3	96.7	87.8	230
EAS (Ours)	89.0	91.3	81.7	81.3	86.7	88.7	83.0	96.7	94.0	96.7	88.9	219
OFA-V	87.7	91.0	80.0	80.0	84.7	89.7	83.0	95.7	93.7	95.3	88.0	278
OFA-T	88.0	90.0	80.0	80.0	86.7	89.3	85.0	95.7	94.3	95.7	88.5	279
EAS (Ours)	90.0	92.0	81.3	80.3	87.7	90.3	84.3	97.3	94.3	96.7	89.4	269
OFA-V	88.3	90.7	81.0	79.7	85.7	90.3	83.7	95.0	92.7	96.7	88.4	329
OFA-T	88.0	90.0	80.0	80.3	86.0	90.0	85.7	95.7	93.7	95.7	88.5	328
EAS (Ours)	89.3	91.7	82.0	82.3	89.0	90.0	84.3	97.3	94.3	96.7	89.7	316
OFA-V	87.0	90.0	80.7	79.7	85.7	90.0	83.7	95.0	93.0	96.7	88.1	364
OFA-T	87.3	91.3	80.0	80.7	87.0	89.3	84.7	96.3	93.3	96.3	88.6	373
EAS (Ours)	88.7	91.7	82.0	82.3	88.7	90.3	85.3	97.3	95.0	97.3	89.9	361

Table II: Comparisons on ImageNet-12. We report the Top-1 Accuracy (Acc.) of different architectures on diverse tasks. “T- t ” indicates the t -th task. “Avg. Acc.” and “Avg. #MAdds” denote the average Top-1 accuracy and the average number of multiply-adds, respectively.

Method	T-1	T-2	T-3	T-4	T-5	T-6	T-7	T-8	T-9	T-10	T-11	T-12	Avg. Acc. (%)	Avg. #MAdds (M)
OFA-V	81.5	86.9	92.9	84.6	87.6	76.5	83.1	79.3	80.8	84.4	80.2	78.0	83.0	229
OFA-T	80.9	86.6	92.5	85.6	88.1	77.4	83.4	79.6	80.8	85.2	79.7	79.1	83.2	229
EAS (Ours)	81.8	86.9	93.1	85.9	88.5	78.4	83.5	79.6	80.9	84.7	79.8	78.1	83.4	223
OFA-V	81.6	87.3	92.7	85.8	88.5	77.4	84.2	79.0	81.1	84.3	80.5	78.6	83.4	279
OFA-T	81.1	87.0	92.6	86.2	89.1	79.1	83.8	79.5	81.3	85.2	80.2	78.5	83.6	279
EAS (Ours)	81.3	87.4	92.9	86.6	88.1	77.8	83.3	79.3	81.9	85.5	80.3	80.0	83.7	266
OFA-V	81.9	86.8	92.3	85.6	88.6	78.3	83.7	79.2	82.4	85.1	80.5	79.0	83.6	328
OFA-T	81.1	87.2	93.0	86.2	89.0	79.3	83.9	79.1	81.1	85.2	80.5	78.8	83.7	329
EAS (Ours)	81.6	87.5	93.0	86.5	89.1	78.6	84.3	79.3	82.3	85.3	80.1	79.6	83.9	320
OFA-V	80.8	87.8	93.3	86.6	88.4	79.2	84.4	79.2	81.5	85.3	80.8	78.8	83.8	376
OFA-T	80.8	87.3	93.3	85.9	89.0	79.6	84.6	79.9	81.7	85.4	80.0	79.0	83.9	379
EAS (Ours)	81.5	87.7	93.3	86.8	89.4	79.2	84.2	80.2	82.0	86.0	80.9	79.9	84.3	358

4 Experiments

Datasets. We evaluate the proposed EAS on the large-scale image classification dataset, namely ImageNet [6]. Based on ImageNet, we construct two datasets for different tasks following [8]. The first dataset, denoted by ImageNet-10, consists of 10 tasks and each task contains 6 classes. The total number of training and testing samples for ImageNet-10 are 77,237 and 3,000, respectively. The second dataset, denoted by ImageNet-12, consists of 12 tasks and each task contains 20 classes. The total number of training and testing samples for ImageNet-12 are 308,494 and 12,000, respectively. For all datasets, we randomly choose 10k training samples as the validation set. More details about the datasets are put in the supplementary material.

Search space. We apply our proposed EAS to MobileNetV3 [19] search space. Specifically, the model is split into 5 units following [2]. We choose the depth of each unit from $\{2, 3, 4\}$, the width expansion ratio of each inverted residual block from $\{3, 4, 6\}$, and the kernel size of each depthwise convolution from $\{3, 5, 7\}$.

Compared methods. We compare our EAS with the state-of-the-art one-shot NAS method OFA [2]. To perform classification on different tasks, we construct the following variants for comparisons. **OFA-V**: the vanilla OFA that trains an over-parameterized network and only performs a single evolutionary search for all tasks. **OFA-T**: trains an over-parameterized network and searches for optimal architectures for each task.

Evaluation metrics. We measure the performance of different methods using the Top-1 accuracy on diverse tasks given a specific budget. Following [49, 19], we measure the computational cost of the searched architectures using the number of multiply-adds (#MAdds). Following [29], we also use the training cost on a GPU device (GeForce RTX 3090) to measure the time of training an architecture generator and the search cost on a CPU device (Intel Xeon Gold 6230R) to measure the time of finding an optimal architecture.

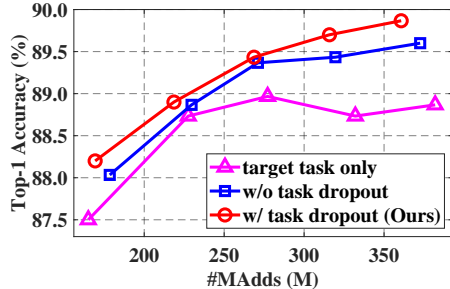


Figure III: Performance comparisons of the proposed EAS with different task dropout strategies on ImageNet-10.

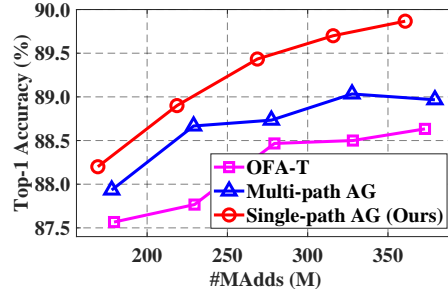


Figure IV: Performance comparisons of the proposed EAS with different search algorithms on ImageNet-10.

Implementation details. We first train an over-parameterized network on all tasks of training data for 120 epochs using the progressive shrinking strategy [2] with a mini-batch size of 256. Different from OFA [2], we share the kernel weights among different kernel sizes without using the kernel transformation. We use SGD with a momentum of 0.9 for optimization [40]. The learning rate starts at 0.01 and decays with cosine annealing [32]. We set the drop rate q to 0.6 and 0.1 for the experiments on ImageNet-10 and ImageNet-12, respectively. We then train the architecture generator for 90 epochs on the validation set. The number of learnable embedding vectors K for the resource budget is set to 10. We set the dimension of the embedding vector to 32 for both the task label and resource budget. We use Adam for optimization [25] with a learning rate of 1×10^{-3} . The hyper-parameters λ and τ are set to 0.01 and 1, respectively. For all experiments on ImageNet-10 and ImageNet-12, we set B_L and B_H to 150 and 550, respectively. We put more implementation details in the supplementary material.

4.1 Main results

We show the results in Table I and Table II. We also put the visualization of the generated architectures in the supplementary materials. Compared with OFA-V, OFA-T achieves better or comparable performance in all tasks with different resource budgets. These results demonstrate that searching architectures for all tasks may not be optimal for each task. Compared with OFA-T, our method achieves better or comparable model accuracy in all tasks with diverse resource budgets. For the average performance of all tasks on different resource budgets, our EAS consistently outperforms OFA-T in terms of the model accuracy with fewer #MAAdds. These results verify the effectiveness of our method. Note that for task-2 of ImageNet-10, the obtained architecture of EAS achieves the best accuracy at the resource budget level of 269 M Avg. #MAAdds. With the increase of #MAAdds, the accuracy of the searched architectures goes worse. Similar results are also observed for the baseline methods, such as task-6 of ImageNet-10 for OFA-T and task-1 of ImageNet-12 for OFA-V. One possible reason is that for those tasks of data that are easy to be classified, using a compact network with low computational overhead is sufficient to obtain promising performance. Increasing the resource budget may suffer from the over-fitting issue.

4.2 Ablation studies

Effectiveness of the task dropout. To investigate the effect of the task dropout strategy, we first train the over-parameterized networks with and without task dropout on ImageNet-10 and then use the proposed architecture generator to obtain architectures. We also train the over-parameterized network with the target task only by setting the drop rate q to 1, which indicates that we completely drop the output logits corresponding to the non-target tasks during training. More results in terms of different drop rates are put in the supplementary material. We report the average Top-1 accuracy and average #MAAdds across all tasks in Figure III. From the results, EAS without task dropout surpasses the one with the target task only, especially at high resource budget settings. These results verify that exploiting the useful context information in other tasks improves the performance on the current task. More critically, EAS with task dropout consistently outperforms the one without task dropout and the performance improvement brought by the task dropout strategy is more significant at higher resource

Table III: Comparisons of the training time and search time for architecture search among different methods on ImageNet-10. The training time for OFA-T is the cost of sampling architecture-accuracy pairs and learning a surrogate model. For the multi-path AG and single-path AG, the training time is the cost of learning an architecture generator. The search time is the cost of finding architectures for 10 tasks and 5 resource budgets.

Method	OFA-T	Multi-path AG	Single-path AG (Ours)
Training Time (GPU hour)	104.0	40.3	0.9
Search Time (CPU second)	3474.1	<0.1	<0.1

budget levels. For example, the architectures obtained by EAS with task dropout have lower #MAdds and surpass those without task dropout by 0.3% on the Top-1 accuracy at the budget level of 320 #MAdds. These results demonstrate the effectiveness of the proposed task dropout strategy.

Effectiveness of the architecture generator. To investigate the effect of the architecture generator, we first train the over-parameterized networks with task dropout on ImageNet-10 and then use the following methods to search the architectures. 1) **OFA-T**: uses the evolutionary algorithm to search optimal architectures for diverse tasks and resources [2]. 2) **Multi-path AG**: based on the proposed architecture generator, we use the multi-path scheme [29, 56] to encode the generated architectures. 3) **Single-path AG**: uses the proposed architecture generator to obtain architectures with the single-path architecture encoding. We report the average Top-1 accuracy and average #MAdds across all tasks in Figure IV. We also show the training cost and search cost in Table III. From the results, the multi-path AG consistently outperforms OFA-T at different levels of #MAdds. Our proposed single-path AG further outperforms the multi-path scheme by a large margin (89.43% vs. 88.73% at the budget level of 277 M Avg. #MAdds), which demonstrates the effectiveness of the proposed architecture generator with the single-path architecture encoding. Moreover, compared with OFA-T, the multi-path AG has a much lower training cost and search cost. More critically, our single-path AG further reduces the training cost, which demonstrates the efficiency of our single-path architecture generator in both training and architecture search. For example, our proposed architecture generator is able to generate architectures within 0.1 second for 50 development requirements.

5 Conclusion and future work

In this paper, we have studied a new challenging problem of efficient deployment for different tasks with various resources, where the tasks of interest (each task corresponds to a group of classes) are dynamically specified at testing time. To this end, we have proposed a novel and general framework, called Elastic Architecture Search (EAS), to instantly specialize neural networks at runtime. The proposed EAS first trains an over-parameterized network with the **task dropout** strategy that randomly drops the output logits corresponding to different tasks. In this way, the over-parameterized network supports many sub-networks for diverse tasks once trained. Based on the well-trained over-parameterized network, we have further proposed an efficient architecture generator to instantly obtain architectures within a single forward pass given arbitrary tasks and budgets during inference. Experiments on two image classification datasets have shown the superiority of the proposed methods under diverse deployment scenarios.

The proposed EAS is able to instantly find an accurate and compact architecture given a deployment scenario at runtime, which brings great social and environmental benefits in terms of significantly saving the financial expenditure for both academia and industry and greatly reducing the carbon emissions for training and deploying deep models in dynamic scenarios. However, it may also bring some negative societal impacts, such as job losses for algorithm engineers. Moreover, improper use of the proposed EAS may result in disastrous effects. For example, obtaining a very small network for an autonomous driving car may bring greater risks to the driver.

In the future, we may extend our method in three aspects. First, we currently perform architecture search based on the given specific task and budget. However, the task label is often unknown in many real-world applications. To address this, we will need to perform task prediction first and then use the proposed method to obtain architectures. Second, we may consider multiple tasks at testing time, which is quite challenging due to the combinatorially large space. For example, for 100 tasks, we have roughly 2^{100} different task combinations. Third, we may extend our proposed method to broader applications, such as dense detection and segmentation, machine translation, etc.

6 Appendix

We organize our supplementary material as follows.

- In Section 6.1, we provide more details about the datasets.
- In Section 6.2, we describe more implementation details about the proposed method and baselines.
- In Section 7, we investigate the effect of different drop rates.
- In Section 7.1, we show the visualization results of the searched architectures.

6.1 More details about the datasets

In this section, we introduce more details about the datasets mentioned in Section 4. Based on ImageNet [6], we construct two datasets for different tasks following [8], namely ImageNet-10 and ImageNet-12. We show more details of ImageNet-10 and ImageNet-12 in Tables IV and V, respectively.

Table IV: More details about ImageNet-10. We report the names of tasks and classes. Each class name is separated by a comma.

Task	Class
Dog	Chihuahua, Japanese spaniel, Maltese dog, Pekinese, Shih-Tzu, Blenheim spaniel
Bird	Cock, Hen, Ostrich, Brambling, Goldfinch, House finch
Insect	Tiger beetle, Ladybug, Ground beetle, Long-horned beetle, Leaf beetle, Dung beetle
Monkey	Guenon, Patas, Baboon, Macaque, Langur, Colobus
Car	Jeep, Limousine, Cab, Beach wagon, Ambulance, Convertible
Cat	Leopard, Snow leopard, Jaguar, Lion, Cougar, Lynx
Truck	Tow truck, Moving van, Fire engine, Pickup, Garbage truck, Police van
Fruit	Granny Smith, Rapeseed, Corn, Acorn, Hip, Buckeye
Fungus	Agaric, Gyromitra, Stinkhorn, Earthstar, Hen-of-the-woods, Coral fungus
Boat	Gondola, Fireboat, Speedboat, Lifeboat, Yawl, Canoe

6.2 More implementation details

In this section, we introduce more implementation details mentioned in Section 4. Following [2, 60], we use the knowledge distillation technique [17] to train the over-parameterized network. Specifically, we take the largest sub-network from the over-parameterized network as the teacher network. We train the teacher network for 120 epochs with a mini-batch size of 256. We use SGD with a momentum of 0.9 for optimization [40]. The weight decay is set to 3×10^{-5} . The learning rate starts at 0.1 and decays with cosine annealing [32]. We do not use the task dropout strategy during training. For OFA-V and OFA-T, we first sample 16K sub-networks with different architectures and measure their accuracies across diverse tasks on the validation set following [2]. We then train the accuracy predictor for 250 epochs using a mini-batch size of 256. We use SGD with momentum for optimization. The momentum term and weight decay are set to 0.9 and 1×10^{-4} , respectively. The learning rate is initialized to 0.1 and decreased to 0 following the cosine function.

7 Effect of different drop rates

To investigate the effect of the task dropout strategy, we first train the over-parameterized networks with different drop rates q on ImageNet-10 and then use the proposed architecture generator to obtain architectures. We report the results in Figure V. From the results, EAS with a drop rate of 0.6 achieves the best performance. For example, at the #MAAdds level of 316 M, the Top-1 accuracy of the proposed EAS with drop rate of 0.6 is 89.7%, which is higher than those with other drop rates. Hence, we set q to 0.6 by default in our experiments on ImageNet-10. Moreover, with the increase of q , the performance of the searched architectures first goes better and then goes worse. These results demonstrate the effectiveness of the proposed task dropout strategy.

Table V: More details about ImageNet-12. We report the names of tasks and classes. Each class name is separated by a comma.

Task	Class
Dog	Chihuahua, Japanese spaniel, Maltese dog, Pekinese, Shih-Tzu, Blenheim spaniel, Papillon, Toy terrier, Rhodesian ridgeback, Afghan hound, Basset, Beagle, Bloodhound, Bluetick, Black-and-tan coonhound, Walker hound, English foxhound, Redbone, Borzoi, Irish wolfhound
Structure	Dam, Altar, Dock, Apiary, Bannister, Barbershop, Barn, Beacon, Boathouse, Bookshop, Brass, Breakwater, Butcher shop, Castle, Chainlink fence, Church, Cinema, Cliff dwelling, Coil, Confectionery
Bird	Cock, Hen, Ostrich, Brambling, Goldfinch, House finch, Junco, Indigo bunting, Robin, Bulbul, Jay, Magpie, Chickadee, Water ouzel, Kite, Bald eagle, Vulture, Great grey owl, African grey, Macaw
Clothing	Cowboy hat, Crash helmet, Abaya, Academic gown, Diaper, Apron, Feather boa, Football helmet, Bathing cap, Bearskin, Fur coat, Bikini, Gown, Bolo tie, Bonnet, Bow tie, Brassiere, Hoopskirt, Cardigan, Christmas stocking
Vehicle	Minivan, Model T, Ambulance, Amphibian, Electric locomotive, Fire engine, Barrow, Forklift, Beach wagon, Freight car, Garbage truck, Bicycle-built-for-two, Go-kart, Half track, Cab, Horse cart, Jeep, Jinrikisha, Limousine, Convertible
Reptile	Loggerhead, Leatherback turtle, Mud turtle, Terrapin, Box turtle, Banded gecko, Common iguana, American chameleon, Whiptail, Agama, Frilled lizard, Alligator lizard, Gila monster, Green lizard, African chameleon, Komodo dragon, African crocodile, American alligator, Triceratops, Thunder snake
Carnivore	Timber wolf, White wolf, Red wolf, Coyote, Dingo, Dhole, African hunting dog, Hyena, Red fox, Kit fox, Arctic fox, Grey fox, Cougar, Lynx, Leopard, Snow leopard, Jaguar, Lion, Tiger, Cheetah
Insect	Tiger beetle, Ladybug, Ground beetle, Long-horned beetle, Leaf beetle, Dung beetle, Rhinoceros beetle, Weevil, Fly, Bee, Ant, Grasshopper, Cricket, Walking stick, Cockroach, Mantis, Cicada, Leafhopper, Lacewing, Dragonfly
Instrument	Cornet, Maraca, Marimba, Accordion, Acoustic guitar, Drum, Electric guitar, Banjo, Oboe, Ocarina, Flute, Organ, Bassoon, French horn, Gong, Grand piano, Harmonica, Harp, Cello, Chime
Food	French loaf, Bagel, Pretzel, Head cabbage, Broccoli, Cauliflower, Zucchini, Spaghetti squash, Acorn squash, Butternut squash, Cucumber, Artichoke, Bell pepper, Cardoon, Mushroom, Strawberry, Orange, Lemon, Fig, Pineapple
Furniture	Cradle, Crib, Medicine chest, Desk, Dining table, Entertainment center, Barber chair, File, Bassinet, Folding chair, Four-poster, Studio couch, Park bench, Bookcase, Table lamp, Throne, Toilet seat, Chiffonier, China cabinet, Rocking chair
Primate	Indri, Orangutan, Gorilla, Chimpanzee, Gibbon, Siamang, Guenon, Patas, Baboon, Macaque, Langur, Colobus, Proboscis monkey, Marmoset, Capuchin, Howler monkey, Titi, Spider monkey, Squirrel monkey, Madagascar cat

7.1 Visualization results of searched architectures

To demonstrate the effectiveness of the proposed method, we first compute the cosine similarity for each pair of the architectures among different tasks under the same #MAdds level on ImageNet-10. Here, we use the one-hot encoding to encode the architecture following [2]. We then compute the

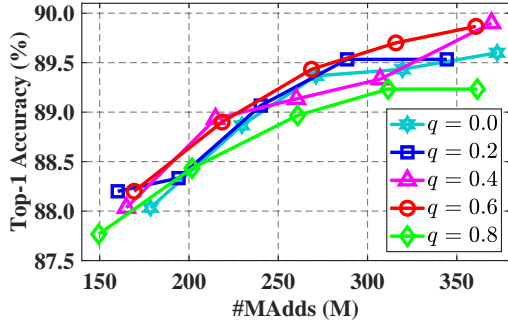


Figure V: Comparisons of the proposed EAS with different drop rates on ImageNet-10.

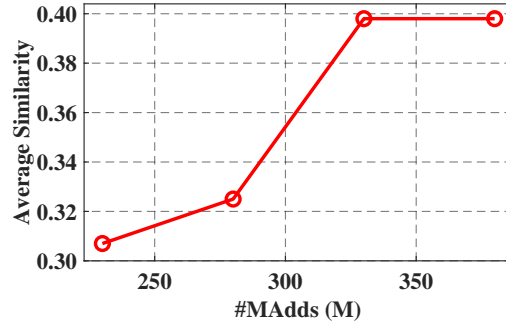


Figure VI: The average architecture cosine similarity vs. #MAdds on ImageNet-10.

average cosine similarity for each of the #MAdds level and report the results in Figure VI. From the results, the average cosine similarity first increases and then saturates with the increase of #MAdds. One possible reason is that the searched network tends to use larger kernel sizes, higher width expansion ratios, and more layers with the increase of #MAdds, which is shown in Figure VII. Therefore, the searched architectures for different tasks become similar with the increase of #MAdds. We further show the searched architectures for different tasks under the same level of #MAdds in Figure VIII. From the results, the searched architectures for different tasks differ a lot, which demonstrates the motivation that the optimal architectures for diverse tasks are different.

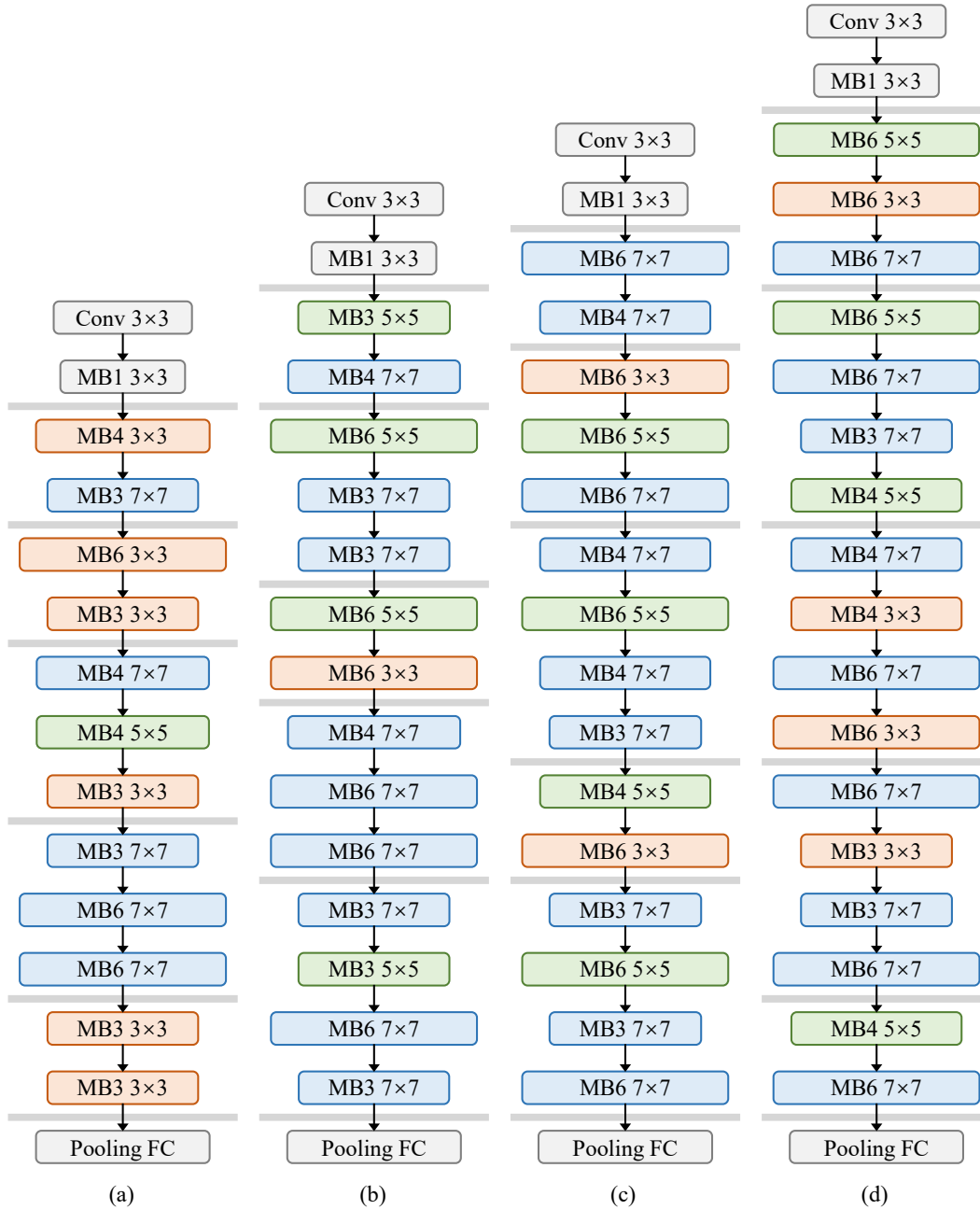


Figure VII: The architectures searched by EAS for T-4 under various resource budgets on ImageNet-10. (a): The searched architecture at the #MAadds level of 216 M. (b): The searched architecture at the #MAadds level of 270 M. (c): The searched architecture at the #MAadds level of 298 M. (d): The searched architecture at the #MAadds level of 370 M.

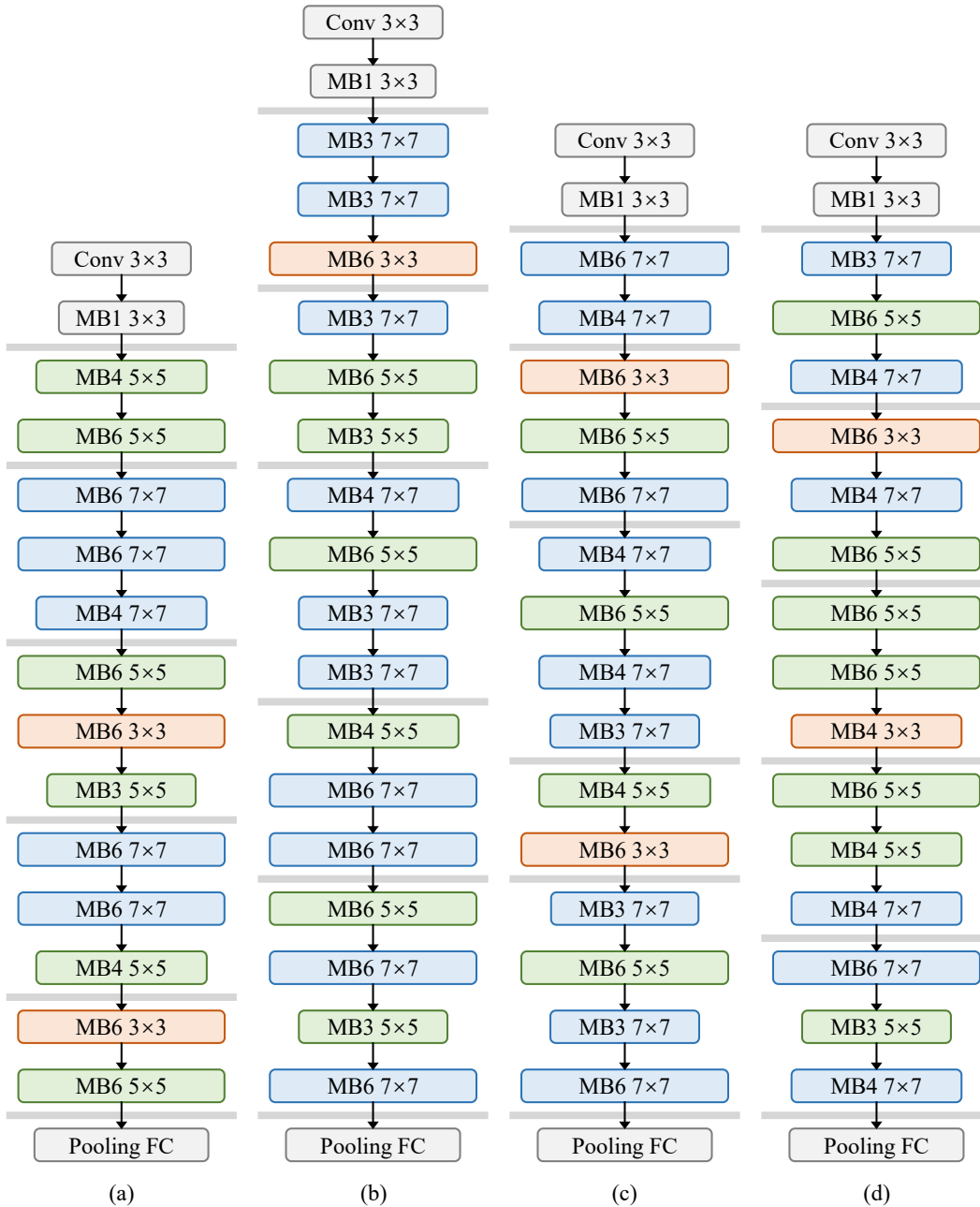


Figure VIII: The architectures searched by EAS at the #MAdds level of 305 M for diverse tasks on ImageNet-10. (a): The searched architecture for T-1. (b) The searched architecture for T-3. (c): The searched architecture for T-4. (d): The searched architecture for T-7.

References

- [1] Y. Bengio, N. Léonard, and A. Courville. Estimating or propagating gradients through stochastic neurons for conditional computation. *arXiv preprint arXiv:1308.3432*, 2013.
- [2] H. Cai, C. Gan, T. Wang, Z. Zhang, and S. Han. Once-for-all: Train one network and specialize it for efficient deployment. In *Proc. Int. Conf. Learn. Repr.*, 2020.
- [3] H. Cai, L. Zhu, and S. Han. ProxylessNAS: Direct neural architecture search on target task and hardware. In *Proc. Int. Conf. Learn. Repr.*, 2019.
- [4] X. Chen, L. Xie, J. Wu, and Q. Tian. Progressive differentiable architecture search: Bridging the depth gap between search and evaluation. In *Proc. IEEE Int. Conf. Comp. Vis.*, pages 1294–1303, 2019.
- [5] A.-C. Cheng, C. H. Lin, D.-C. Juan, W. Wei, and M. Sun. Instanas: Instance-aware neural architecture search. In *Proc. AAAI Conf. on Arti. Intel.*, pages 3577–3584, 2020.
- [6] J. Deng, W. Dong, R. Socher, L.-J. Li, K. Li, and L. Fei-Fei. Imagenet: A large-scale hierarchical image database. In *Proc. IEEE Conf. Comp. Vis. Patt. Recogn.*, pages 248–255, 2009.
- [7] E. L. Denton, W. Zaremba, J. Bruna, Y. LeCun, and R. Fergus. Exploiting linear structure within convolutional networks for efficient evaluation. In *Proc. Adv. Neural Inf. Process. Syst.*, pages 1269–1277, 2014.
- [8] L. Engstrom, A. Ilyas, S. Santurkar, and D. Tsipras. Robustness (python library), 2019.
- [9] S. K. Esser, J. L. McKinstry, D. Bablani, R. Appuswamy, and D. S. Modha. Learned step size quantization. In *Proc. Int. Conf. Learn. Repr.*, 2020.
- [10] H. Fan, Z. Xu, L. Zhu, C. Yan, J. Ge, and Y. Yang. Watching a small portion could be as good as watching all: Towards efficient video classification. In *Proc. Int. Joint Conf. Artif. Intell.*, pages 705–711, 2018.
- [11] S. Guo, Y. Wang, Q. Li, and J. Yan. Dmcp: Differentiable markov channel pruning for neural networks. In *Proc. IEEE Conf. Comp. Vis. Patt. Recogn.*, pages 1536–1544, 2020.
- [12] Y. Guo, Y. Chen, Y. Zheng, Q. Chen, P. Zhao, J. Chen, J. Huang, and M. Tan. Pareto-frontier-aware neural architecture generation for diverse budgets. *arXiv preprint arXiv:2103.00219*, 2021.
- [13] Y. Guo, Y. Chen, Y. Zheng, P. Zhao, J. Chen, J. Huang, and M. Tan. Breaking the curse of space explosion: Towards efficient nas with curriculum search. In *Proc. Int. Conf. Mach. Learn.*, pages 3822–3831, 2020.
- [14] Y. Guo, Y. Zheng, M. Tan, Q. Chen, J. Chen, P. Zhao, and J. Huang. Nat: Neural architecture transformer for accurate and compact architectures. In *Proc. Adv. Neural Inf. Process. Syst.*, pages 735–747, 2019.
- [15] Z. Guo, X. Zhang, H. Mu, W. Heng, Z. Liu, Y. Wei, and J. Sun. Single path one-shot neural architecture search with uniform sampling. In *Proc. Eur. Conf. Comp. Vis.*, pages 544–560, 2020.
- [16] K. He, X. Zhang, S. Ren, and J. Sun. Deep residual learning for image recognition. In *Proc. IEEE Conf. Comp. Vis. Patt. Recogn.*, pages 770–778, 2016.
- [17] G. Hinton, O. Vinyals, and J. Dean. Distilling the knowledge in a neural network. *arXiv preprint arXiv:1503.02531*, 2015.
- [18] G. E. Hinton, N. Srivastava, A. Krizhevsky, I. Sutskever, and R. Salakhutdinov. Improving neural networks by preventing co-adaptation of feature detectors. *arXiv preprint arXiv:1207.0580*, 2012.
- [19] A. Howard, M. Sandler, G. Chu, L.-C. Chen, B. Chen, M. Tan, W. Wang, Y. Zhu, R. Pang, V. Vasudevan, et al. Searching for mobilenetv3. In *Proc. IEEE Int. Conf. Comp. Vis.*, pages 1314–1324, 2019.
- [20] A. G. Howard, M. Zhu, B. Chen, D. Kalenichenko, W. Wang, T. Weyand, M. Andreetto, and H. Adam. Mobilenets: Efficient convolutional neural networks for mobile vision applications. *arXiv preprint arXiv:1704.04861*, 2017.
- [21] G. Huang, D. Chen, T. Li, F. Wu, L. van der Maaten, and K. Q. Weinberger. Multi-scale dense networks for resource efficient image classification. In *Proc. Int. Conf. Learn. Repr.*, 2018.
- [22] S.-Y. Huang and W.-T. Chu. Searching by generating: Flexible and efficient one-shot nas with architecture generator. In *Proc. IEEE Conf. Comp. Vis. Patt. Recogn.*, 2021.
- [23] M. Jaderberg, A. Vedaldi, and A. Zisserman. Speeding up convolutional neural networks with low rank expansions. In *Proc. Brit. Mach. Vis. Conf.*, 2014.
- [24] E. Jang, S. Gu, and B. Poole. Categorical reparameterization with gumbel-softmax. In *Proc. Int. Conf. Learn. Repr.*, 2017.
- [25] D. P. Kingma and J. Ba. Adam: A method for stochastic optimization. In *Proc. Int. Conf. Learn. Repr.*, 2015.
- [26] Y. Li, X. Dong, and W. Wang. Additive powers-of-two quantization: An efficient non-uniform discretization for neural networks. In *Proc. Int. Conf. Learn. Repr.*, 2020.

- [27] Y. Li, G. Hu, Y. Wang, T. Hospedales, N. M. Robertson, and Y. Yang. Differentiable automatic data augmentation. In *Proc. Eur. Conf. Comp. Vis.*, pages 580–595, 2020.
- [28] J. Lin, Y. Rao, J. Lu, and J. Zhou. Runtime neural pruning. In *Proc. Adv. Neural Inf. Process. Syst.*, pages 2181–2191, 2017.
- [29] H. Liu, K. Simonyan, and Y. Yang. DARTS: differentiable architecture search. In *Proc. Int. Conf. Learn. Repr.*, 2019.
- [30] J. Liu, B. Zhuang, Z. Zhuang, Y. Guo, J. Huang, J. Zhu, and M. Tan. Discrimination-aware network pruning for deep model compression. *IEEE Trans. Pattern Anal. Mach. Intell.*, 2021.
- [31] Z. Liu, M. Sun, T. Zhou, G. Huang, and T. Darrell. Rethinking the value of network pruning. In *Proc. Int. Conf. Learn. Repr.*, 2019.
- [32] I. Loshchilov and F. Hutter. SGDR: stochastic gradient descent with warm restarts. In *Proc. Int. Conf. Learn. Repr.*, 2017.
- [33] Z. Lu, K. Deb, E. D. Goodman, W. Banzhaf, and V. N. Boddeti. Nsganetv2: Evolutionary multi-objective surrogate-assisted neural architecture search. In *Proc. Eur. Conf. Comp. Vis.*, pages 35–51, 2020.
- [34] Z. Lu, I. Whalen, V. Boddeti, Y. D. Dhebar, K. Deb, E. D. Goodman, and W. Banzhaf. Nsga-net: neural architecture search using multi-objective genetic algorithm. In *Proc. Genetic Evol. Comp. Conf.*, pages 419–427, 2019.
- [35] C. J. Maddison, A. Mnih, and Y. W. Teh. The concrete distribution: A continuous relaxation of discrete random variables. In *Proc. Int. Conf. Learn. Repr.*, 2017.
- [36] P. Molchanov, S. Tyree, T. Karras, T. Aila, and J. Kautz. Pruning convolutional neural networks for resource efficient inference. In *Proc. Int. Conf. Learn. Repr.*, 2017.
- [37] W. Park, D. Kim, Y. Lu, and M. Cho. Relational knowledge distillation. In *Proc. IEEE Conf. Comp. Vis. Patt. Recogn.*, pages 3967–3976, 2019.
- [38] B. Peng, W. Tan, Z. Li, S. Zhang, D. Xie, and S. Pu. Extreme network compression via filter group approximation. In *Proc. Eur. Conf. Comp. Vis.*, pages 307–323, 2018.
- [39] H. Pham, M. Y. Guan, B. Zoph, Q. V. Le, and J. Dean. Efficient neural architecture search via parameter sharing. In *Proc. Int. Conf. Mach. Learn.*, pages 4092–4101, 2018.
- [40] N. Qian. On the momentum term in gradient descent learning algorithms. *Neural Netw.*, pages 145–151, 1999.
- [41] A. Radford, L. Metz, and S. Chintala. Unsupervised representation learning with deep convolutional generative adversarial networks. In *Proc. Int. Conf. Learn. Repr.*, 2016.
- [42] E. Real, A. Aggarwal, Y. Huang, and Q. V. Le. Regularized evolution for image classifier architecture search. In *Proc. AAAI Conf. on Arti. Intel.*, pages 4780–4789, 2019.
- [43] E. Real, S. Moore, A. Selle, S. Saxena, Y. L. Suematsu, J. Tan, Q. V. Le, and A. Kurakin. Large-scale evolution of image classifiers. In *Proc. Int. Conf. Mach. Learn.*, pages 2902–2911, 2017.
- [44] A. Recasens, P. Kellnhofer, S. Stent, W. Matusik, and A. Torralba. Learning to zoom: a saliency-based sampling layer for neural networks. In *Proc. Eur. Conf. Comp. Vis.*, pages 52–67, 2018.
- [45] M. Ren, A. Pokrovsky, B. Yang, and R. Urtasun. Sbnnet: Sparse blocks network for fast inference. In *Proc. IEEE Conf. Comp. Vis. Patt. Recogn.*, pages 8711–8720, 2018.
- [46] S. Ren, K. He, R. B. Girshick, and J. Sun. Faster R-CNN: towards real-time object detection with region proposal networks. *IEEE Trans. Pattern Anal. Mach. Intell.*, pages 1137–1149, 2017.
- [47] A. Romero, N. Ballas, S. E. Kahou, A. Chassang, C. Gatta, and Y. Bengio. Fitnets: Hints for thin deep nets. In *Proc. Int. Conf. Learn. Repr.*, 2015.
- [48] R. Ru, P. M. Esperança, and F. M. Carlucci. Neural architecture generator optimization. In *Proc. Adv. Neural Inf. Process. Syst.*, 2020.
- [49] M. Sandler, A. Howard, M. Zhu, A. Zhmoginov, and L.-C. Chen. Mobilenetv2: Inverted residuals and linear bottlenecks. In *Proc. IEEE Conf. Comp. Vis. Patt. Recogn.*, pages 4510–4520, 2018.
- [50] D. Stamoulis, R. Ding, D. Wang, D. Lymberopoulos, B. Priyantha, J. Liu, and D. Marculescu. Single-path NAS: designing hardware-efficient convnets in less than 4 hours. In *Eur. Conf. Mach. Learn. Princ. Pract. Knowl. Discovery in Databases*, pages 481–497, 2019.
- [51] D. Stamoulis, R. Ding, D. Wang, D. Lymberopoulos, B. Priyantha, J. Liu, and D. Marculescu. Single-path mobile automl: Efficient convnet design and NAS hyperparameter optimization. *IEEE J. Sel. Top. Signal Process.*, pages 609–622, 2020.
- [52] M. Tan, B. Chen, R. Pang, V. Vasudevan, M. Sandler, A. Howard, and Q. V. Le. Mnasnet: Platform-aware neural architecture search for mobile. In *Proc. IEEE Conf. Comp. Vis. Patt. Recogn.*, pages 2820–2828, 2019.

- [53] L. Wan, M. D. Zeiler, S. Zhang, Y. LeCun, and R. Fergus. Regularization of neural networks using dropconnect. In *Proc. Int. Conf. Mach. Learn.*, pages 1058–1066, 2013.
- [54] X. Wang, F. Yu, Z.-Y. Dou, T. Darrell, and J. E. Gonzalez. Skipnet: Learning dynamic routing in convolutional networks. In *Proc. Eur. Conf. Comp. Vis.*, pages 420–436, 2018.
- [55] Y. Wang, K. Lv, R. Huang, S. Song, L. Yang, and G. Huang. Glance and focus: a dynamic approach to reducing spatial redundancy in image classification. In *Proc. Adv. Neural Inf. Process. Syst.*, 2020.
- [56] B. Wu, X. Dai, P. Zhang, Y. Wang, F. Sun, Y. Wu, Y. Tian, P. Vajda, Y. Jia, and K. Keutzer. Fbnet: Hardware-aware efficient convnet design via differentiable neural architecture search. In *Proc. IEEE Conf. Comp. Vis. Patt. Recogn.*, pages 10734–10742, 2019.
- [57] W. Wu, D. He, X. Tan, S. Chen, Y. Yang, and S. Wen. Dynamic inference: A new approach toward efficient video action recognition. In *Proc. IEEE Conf. Comp. Vis. Patt. Recogn. Workshops*, pages 2890–2898, 2020.
- [58] Z. Wu, C. Xiong, Y.-G. Jiang, and L. S. Davis. Liteeval: A coarse-to-fine framework for resource efficient video recognition. In *Proc. Adv. Neural Inf. Process. Syst.*, pages 7778–7787, 2019.
- [59] S. Xie, A. Kirillov, R. B. Girshick, and K. He. Exploring randomly wired neural networks for image recognition. In *Proc. IEEE Int. Conf. Comp. Vis.*, pages 1284–1293, 2019.
- [60] J. Yu and T. S. Huang. Universally slimmable networks and improved training techniques. In *Proc. IEEE Int. Conf. Comp. Vis.*, pages 1803–1811, 2019.
- [61] J. Yu, P. Jin, H. Liu, G. Bender, P.-J. Kindermans, M. Tan, T. Huang, X. Song, R. Pang, and Q. Le. Bignas: Scaling up neural architecture search with big single-stage models. In *Proc. Eur. Conf. Comp. Vis.*, pages 702–717, 2020.
- [62] X. Yu, T. Liu, X. Wang, and D. Tao. On compressing deep models by low rank and sparse decomposition. In *Proc. IEEE Conf. Comp. Vis. Patt. Recogn.*, pages 67–76, 2017.
- [63] S. Zagoruyko and N. Komodakis. Paying more attention to attention: Improving the performance of convolutional neural networks via attention transfer. In *Proc. Int. Conf. Learn. Repr.*, 2017.
- [64] S. Zhou, Y. Wu, Z. Ni, X. Zhou, H. Wen, and Y. Zou. Dorefa-net: Training low bitwidth convolutional neural networks with low bitwidth gradients. *arXiv preprint arXiv:1606.06160*, 2016.
- [65] B. Zhuang, C. Shen, M. Tan, L. Liu, and I. Reid. Towards effective low-bitwidth convolutional neural networks. In *CVPR*, pages 7920–7928, 2018.
- [66] Z. Zhuang, M. Tan, B. Zhuang, J. Liu, Y. Guo, Q. Wu, J. Huang, and J. Zhu. Discrimination-aware channel pruning for deep neural networks. In *Proc. Adv. Neural Inf. Process. Syst.*, pages 883–894, 2018.
- [67] B. Zoph and Q. V. Le. Neural architecture search with reinforcement learning. In *Proc. Int. Conf. Learn. Repr.*, 2017.